

Analysis of Suspended Solids in Water Using Remotely Sensed High Resolution Derivative Spectra

Abstract

Discrimination of the chlorophyll signal from those of suspended sediments and the water itself has proven to be a difficult problem in optical remote sensing of algal biomass. Our study uses numerical differentiation of high resolution spectral data collected at close range over experimental tanks to address this problem. Results indicate that pure water effects can be reduced by a first-order derivative curve and suspended sediment effects can be removed by a second-order transformation. Chlorophyll content is correlated with the difference between the second derivatives at 660 and 695 nanometres. This relationship holds even in the presence of background turbidity. Thus, it is an effective means of compensating for interference from suspended solids. Our findings are discussed as they relate to the use of remote sensing for lake and reservoir management.

Introduction

Remote sensing technology has been used extensively to detect and quantify water quality parameters in natural water bodies and reservoirs (Horn and Morrissey, 1984; Verdin, 1985; Jensen *et al.*, 1989). Sensors with a wide variety of spectral, spatial, and temporal resolutions, mounted on an assortment of platforms including satellites and aircraft, have been used to evaluate chemical pollutants, suspended solids, and chlorophyll abundance. One of the most persistent problems in remote sensing of suspended solids (including organic solids) in water is discriminating the effects of turbidity due to suspended sediments from those of algal chlorophyll. This is particularly significant in lakes and reservoirs because levels of algal chlorophyll are an indicator of trophic condition and an indirect indicator of other important management concerns such as pollution by agricultural fertilizers, pesticides, and herbicides (Alfoldi, 1982; DeNoyelles *et al.*, 1982). Low resolution imaging spectroradiometers such as those on the Landsat satellites are optimized for examining terrestrial rather than aquatic systems (Hilton, 1984), and are, therefore, less than ideal for addressing this problem. In particular, Landsat sensors record data in only a few broad spectral bands, the resolution of which are too coarse to detect much of the spectral "fine structure" associated with suspended solids in water.

Aircraft-mounted high resolution imaging spectrometers such as the Advanced Visible/Infrared Imaging Spectrometer (AVIRIS), with 224 narrow contiguous bands ranging from 400 to 2400 nanometres (nm), are capable of detecting spectral

fine structure, and offer improved capability for separating the effects of sedimentary turbidity from algal chlorophyll in water. Discriminating the effects of these two substances, however, remains a significant problem even for instruments of high spectral resolution. Quibel (1991) suggested that the difference between the reflectance peak at 710 nm and the trough at 660 nm in algae-laden waters remained roughly constant with increasing suspended sediment content and could, therefore, be used to gauge algae content despite variable turbidity. Demetriades-Shah *et al.* (1990) proposed the use of derivative spectra to separate the effects of "vegetation foreground" from "soil background" in spectra of agricultural crops. This technique has been used extensively in analytical chemistry to enhance minor components within a composite spectrum (Martin, 1957; Green and O'Hare, 1974). Demetriades-Shah *et al.* suggested that it should be possible to decompose other composite signals, including turbid water, using this method. Our research investigates the use of derivative spectra for separating the effects of turbidity and chlorophyll in data acquired by means of high-resolution spectrometry.

Derivative Spectra

Spectral reflectance from a volume of water in a turbid lake or reservoir can be conceptualized as a composite signal representing the weighted sum of the three components: water, suspended sediments, and suspended algal chlorophyll. The reflection from the target can thus be summarized as

$$R = W_w r_w + W_t r_t + W_c r_c \quad (1)$$

where

- R = composite volume reflectance from all sources;
 r_w , r_t , and r_c = reflectance from water, turbidity, and chlorophyll components; and
 W_w , W_t , W_c = the weighting of each component.

Each component has a distinctive spectral pattern or signa-

Douglas G. Goodin*, Luoheng Han, Rolland N. Fraser, Donald C. Rundquist, and Wesley A. Stebbins
 Center for Advanced Land Management Information Technologies, Conservation and Survey Division, Institute of Agriculture and Natural Resources, University of Nebraska - Lincoln, Lincoln, NE 68588-0517

John F. Schalles
 Department of Biology, Creighton University, Omaha, NE 68178

Photogrammetric Engineering & Remote Sensing,
 Vol. 59, No. 4, April 1993, pp. 505-510.

0099-1112/93/5904-505\$03.00/0

©1993 American Society for Photogrammetry and Remote Sensing

*Presently with the Department of Geography, Kansas State University, Dickens Hall, Manhattan, KS 66506-0801.

ture, and the blending of these patterns produces the spectral signature for turbid water.

Each component of the composite signal can be represented by an N^{th} order polynomial. If N varies for the individual components, then successive differentiation of the original (0th order) composite curve should systematically remove the lower-order effects.

To demonstrate the effect of successive differentiation on a turbid water spectrum, consider the zero-, first-, and second-order spectra for clear water, turbid water, and algal chlorophyll with turbidity in water (Figures 1, 2, and 3, respectively, data collected by the methods described below). The zero-order (or reflectance) spectrum for clear water (Figure 1) shows higher reflectance in the visible wavebands (400 to 700 nm), peaking at about 500 nm, but very little reflectance in the near-infrared (700 to 900 nm), a portion of the spectrum strongly absorbed by liquid water (Curcio and Petty, 1951). Both the first- and second-order curves are virtually zero at all wavelengths. From this, we may conclude that most of the spectral effects of water reflection are effectively negated by the first derivative. Reflection from clear water can, therefore, be considered a first-order effect. Similarly, Figure 2 suggests that turbidity is a second-order effect, because the first-order spectral signature for turbid water exhibits a characteristic trough or depression centered at approximately 720 nm and the second differentiation of the curve negates this effect.

The zero-order spectral signature for algal chlorophyll combined with turbidity in water (Figure 3) is more complex than either clear or turbid water. In the visible region, a peak in the green spectrum (500 to 600 nm) which is specific to chlorophyll is prominent. The zero-order curve also shows a strong reflection peak at the red/near-infrared boundary (≈ 700 nm), which is reduced further into the infrared. The first-order curve shows a peak at approximately 530 nm and a distinctive peak-and-trough pattern between 680 and 750 nm. More significantly, the second-order curve continues to show a regular pattern of peak and trough at 660 and 710 nm. This indicates that the first-order turbidity effects have been removed (see above discussion), and the remaining effect is specific only to algal chlorophyll. The effects are not as apparent when all three curves are shown on the same axes due to a reduction in the magnitude of the derivatives with each successive differentiation. Later, several curves are

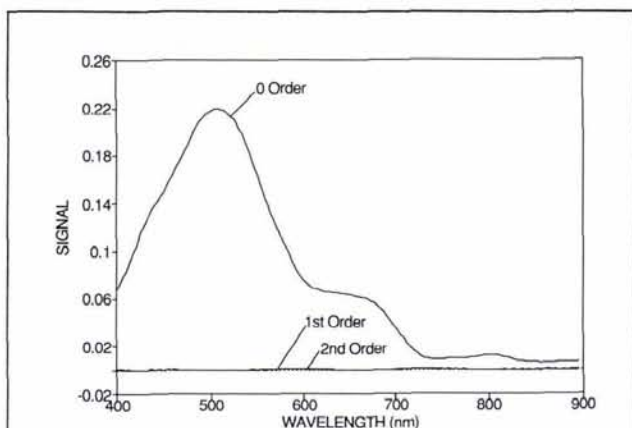


Figure 1. Zero-, first-, and second-order curves for water with no suspended solids.

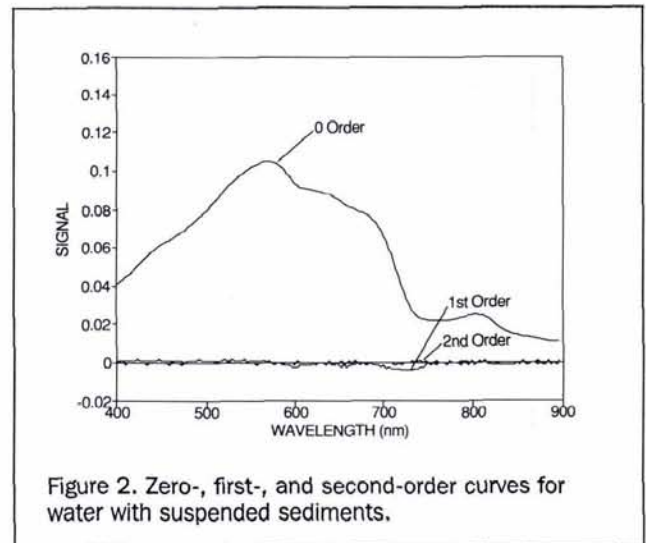


Figure 2. Zero-, first-, and second-order curves for water with suspended sediments.

presented with an enlarged scale which clearly shows this pattern.

Methodology

From the above discussion, it seems evident that water effects can be removed by the first derivative and turbidity effects by the second, leaving a curve consisting only of features associated with chlorophyll. We tested this hypothesis with data collected using high resolution close-range remote sensing over experimental tanks with controlled chlorophyll and turbidity conditions. Use of close-range instruments enables spectral effects to be evaluated without the confounding effects of the atmosphere and viewing geometry encountered with aircraft or satellite data sets.

The tanks used in these experiments were circular, with a diameter of 3.5 m and a depth of 0.85 m. They were lined with 0.15 mil black plastic to reduce internal reflection. Spectral data were collected using a Spectron Industries SE-590 portable spectrometer suspended over the tanks on a truck-mounted telescoping aluminum boom at a height of ap-

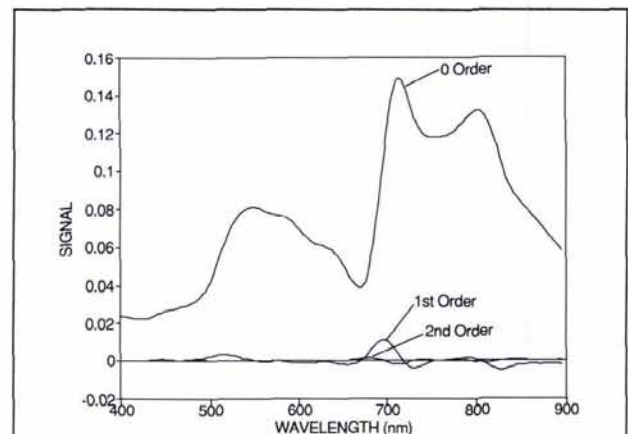


Figure 3. Zero-, first-, and second-order curves for water with suspended sediments and algal chlorophyll.

proximately 3.5 metres above the water surface. A 15° field-of-view optic was fitted to the spectroradiometer, giving an instantaneous field of view on the water surface of about 1.0 m². The SE-590 collects data in 252 discrete, contiguous bands with a nominal bandwidth of 2.96 nm and spectral range of 358 to 1137 nm. In this analysis, only data between 400 and 900 nm were used. The Spectron instrument was interfaced to an IBM compatible microcomputer for control and data-logging. In all experiments, the truck was oriented east-west with the instrument package pointed south to minimize the effects of shadowing in the target area.

The procedure for data collection varied according to the effect being investigated. Reflectance spectra in all experiments were obtained by first scanning the target (the tank surface) at regular intervals, then calibrating over a BaSO₄ panel. Target and calibration scans were then ratioed according to

$$R_i = \frac{r_{ti}}{r_{ci}} W_i \quad (2)$$

where

- R_i = reflectance in band i ,
- r_{ti} = radiance from the target in band i ,
- r_{ci} = radiance from the calibration panel in band i , and
- W_i = factor to correct for non-Lambertian reflectance from calibration panel in band i ,

to calculate reflectance factors for each spectral band. Suspended-sediment data were collected by filling the tank with clean water and introducing measured quantities of sediments at fixed time intervals, then scanning following the sequence described above. Water samples were taken periodically throughout the experiment, and suspended-sediment concentration was determined using a Hach model 2100A turbidimeter calibrated in Nephelometric Turbidity Units (NTUs). A high correlation ($r > 0.90$) existed between our measured turbidity values (NTUs) and total suspended particulate concentrations. Spectra of algal chlorophyll at varying concentrations were obtained by first stimulating an algal bloom by fertilization, then diluting it with freshwater while making sequential spectral scans. Periodic samples were taken and analyzed for chlorophyll biomass using filtration on glass fiber filters. Pigment was extracted from the filtrate with 90 percent buffered acetone and analyzed spectrophotometrically, with acid correction for degraded phaeophytin (APHA, 1989). The spectral effects of chlorophyll with a suspended-sediment background were investigated by introducing measured amounts of sediments into a tank with an existing algal bloom and scanning after each treatment. Periodic sampling was used to determine both suspended sediment load and chlorophyll concentration. As before, reflectance was calculated using Equation 2. In all experiments, solid material suspension was maintained by stirring.

Derivative curves were calculated from reflectance spectra using a seven-point numerical differentiation technique derived from the LaGrangian interpolation polynomial. This method estimates the derivatives at both endpoints and the midpoint of any seven points, as long as the points are contiguous and evenly spaced (Burden and Faires, 1989). The interpolation algorithm uses three related formulas, one for each endpoint and one for the midpoint: i.e.,

$$f'(x_0) = \frac{1}{60h} [-147f(x_0) + 360f(x_1) - 450f(x_2) + 400f(x_3) - 225f(x_4) + 72f(x_5) - 10f(x_6)] \quad (3a)$$

$$f'(x_3) = \frac{-36f(x_0)}{2160h} + \frac{36f(x_1)}{240h} - \frac{36f(x_2)}{48h} + \frac{36f(x_4)}{48h} - \frac{36f(x_5)}{240h} + \frac{36f(x_6)}{2160h} \quad (3b)$$

$$f'(x_6) = \frac{1}{60h} [10f(x_0) - 72f(x_1) + 225f(x_2) - 400f(x_3) + 450f(x_4) - 360f(x_5) + 147f(x_6)] \quad (3c)$$

The terms $f(x_0)$ through $f(x_6)$ represent the reflectance values at the seven points, with $f(x_0)$ and $f(x_6)$ being the left and right endpoints, respectively; $f(x_3)$ the midpoint; and h the distance between the points. An algorithm was developed which applied these equations sequentially over a zero-order reflectance curve, creating a first-order curve consisting of derivatives calculated at each spectral band value. Second-

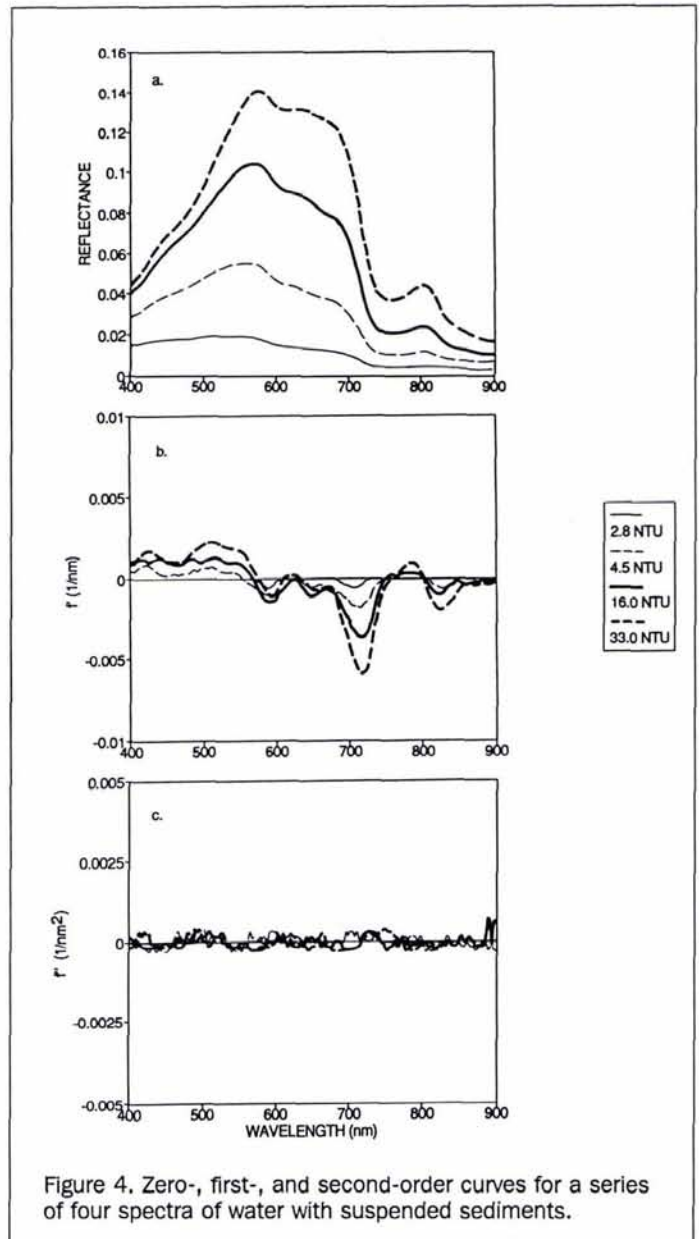


Figure 4. Zero-, first-, and second-order curves for a series of four spectra of water with suspended sediments.

order curves were calculated by applying the same algorithm to a first-order curve. Because differentiation tends to magnify the effects of high-frequency noise in the spectra, a seven-point moving average smoothing filter was passed over the data prior to calculating derivatives. When second-order curves were used, they were calculated from smoothed first-order curves.

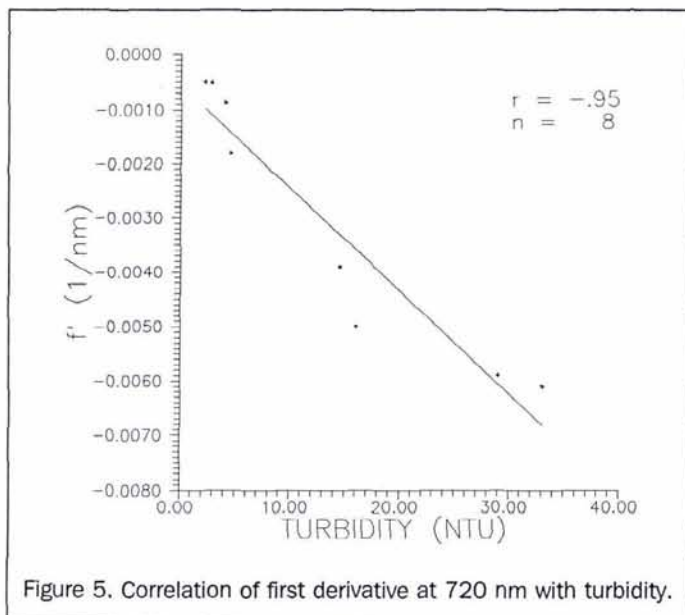
Results and Discussion

Figures 4a, 4b, and 4c show the zero-order reflectance and first- and second-order curves for sedimentary turbidity at four concentrations. For clarity of illustration, only four curves from the full data sets are plotted. Figure 4a clearly shows the increased reflectance from the water as turbidity increases, as well as a broadening of the peak as it shifts to longer wavelengths. Notice also that, although the general shape of the curve remains constant, the distance from peaks to troughs and the slope of the curve in between them increases with increasing concentration. Because, mathematically, derivatives are related to the rate of change, these differences will determine the shape of the derivative curves.

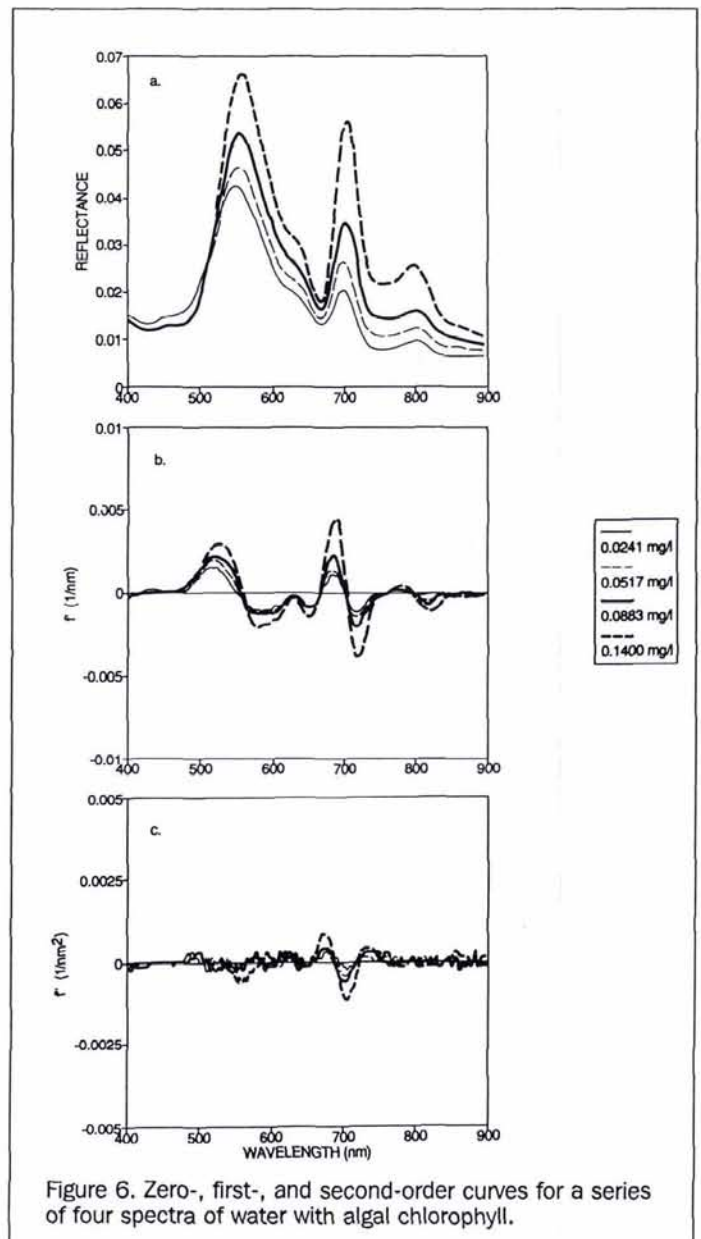
Figure 4b shows that first derivatives for curves with higher turbidity concentrations generally have higher absolute values throughout the spectrum, but show a particularly orderly pattern at about 720 nm. Figure 4c supports the contention that a second differentiation of the turbidity curves removes the effects of suspended solids. The second-order curve shows only very small derivative values and no orderly pattern or structure which can be attributed to conditions in the water.

Figure 5 shows the results of correlating suspended sediment concentration with the absolute value of the first derivative at the 720-nm trough for all eight scans in the data set. The high correlation coefficient ($r = -0.95$, $p < 0.0001$) indicates that this feature is strongly related to sediment concentration.

Figures 6a through 6c illustrate a series of curves similar to those in Figure 4 but with only algal material in the tank. As described in the methodology section, chlorophyll concentration was systematically reduced by diluting the tank



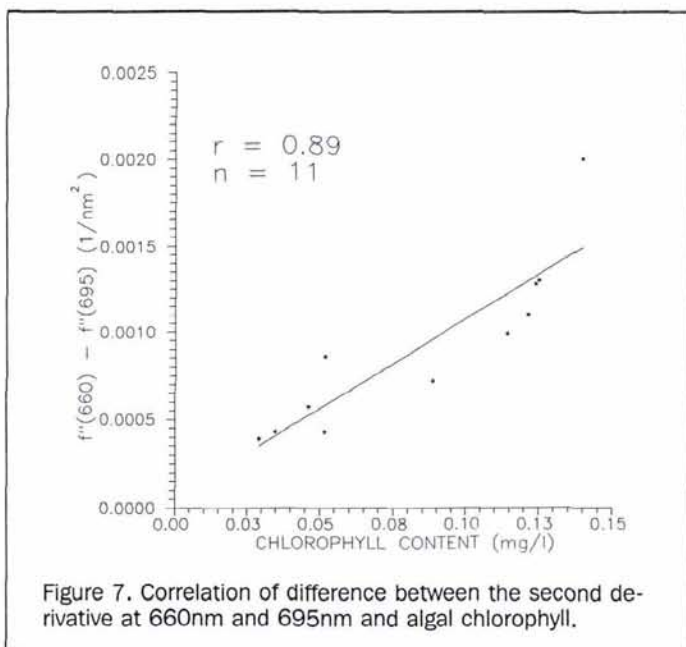
with pure water while a series of scans were taken. The overall pattern of reflectivity change is similar to those shown by the turbidity curves, with higher values at larger chlorophyll concentrations. The first-order curves show a well-defined peak-and-trough pattern in the spectral region between 670 and 750 nm. Comparison of Figures 4b and 6b indicates that, while chlorophyll shows a very distinctive pattern in this region, the trough occurs at nearly the same location as the trough feature in the turbidity curves, making the first-order curve less effective as a means to discriminate between the effects of the two components. The second-order curve also shows a peak-and-trough pattern, but the minima and maxima occur in slightly different places. Correlation between the difference of the minima and maxima and chlorophyll concentration indicates a relationship ($r = 0.89$, $p > 0.001$), although not as strong as the one seen in the turbidity data (see Figure 7).



The effects of differentiation on composite turbidity-chlorophyll spectra are shown in Figure 8. The reflectance curves (Figure 8a) show a transition from a single, well defined reflectance peak at 550 nm at lower turbidity values to a broader, more flat-topped peak extending from 550 to 650 nm at higher turbidity levels. This results from the masking of the chlorophyll green peak by suspended sediments. The peak at about 710 nm, however, remains well-defined in all cases, as does the chlorophyll-a absorption trough at 670 to 680 nm. The first-order curve (Figure 8b) shows systematic increase in absolute value with increasing sediment content at ≈ 720 nm, but the second-order curves, although somewhat "noisy," remain essentially constant at all suspended-sediment concentrations. Because, according to the above discussion, the 720-nm region should respond only to changes in algal chlorophyll concentration, and the algal chlorophyll content of the tank was roughly constant throughout the experiment, this finding supports the supposition that second-order derivative spectra can effectively be used to filter the effects of suspended sediments from composite spectral signatures. Our conclusion is further supported by comparing the difference of the second derivative minima and maxima (at 660 and 695 nm) to the difference between the reflectance at 665 nm and 710 nm suggested by Quibel (1990), as an index of chlorophyll content. Figure 9 shows that, while the appearance of the two curves are similar, at lower turbidity levels the difference in second derivative extrema are flatter, and therefore a superior index of chlorophyll content.

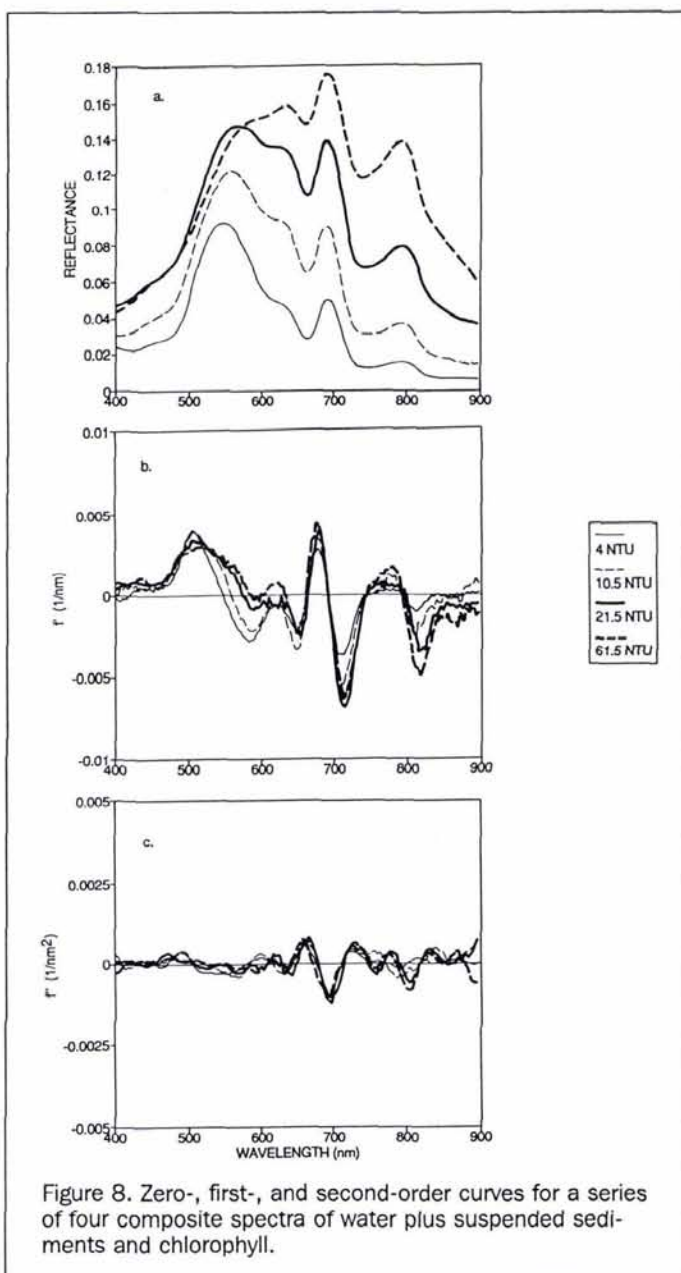
Summary and Conclusions

Derivative spectra have been shown to be an effective technique for separating the contribution of the various components of the composite spectrum of water with suspended solids. Second-order derivatives are especially well suited to discriminating the effects of algal chlorophyll from those of suspended sediments, especially at lower turbidity levels. In particular, the difference between the second derivatives at 660 nm and 695 nm shows a strong relationship with chloro-



phyll content. It is uncertain whether there is a unique relationship between this difference and measured chlorophyll concentration. If there is no unique relationship, relative levels of chlorophyll concentration can be obtained directly from remotely sensed data. If absolute values are required, some field sampling must be done in order to establish a measurement scale. Further research into the relationship between this difference index and chlorophyll content, and additional investigation of other possible relationships between first-, second-, or higher-order derivatives and water quality conditions, is warranted.

High spectral resolution imaging systems mounted on aircraft are currently available, and in the future similar satellite-borne instruments will provide routine high spectral resolution imagery for almost the entire Earth's surface. The availability of these systems provides resource managers



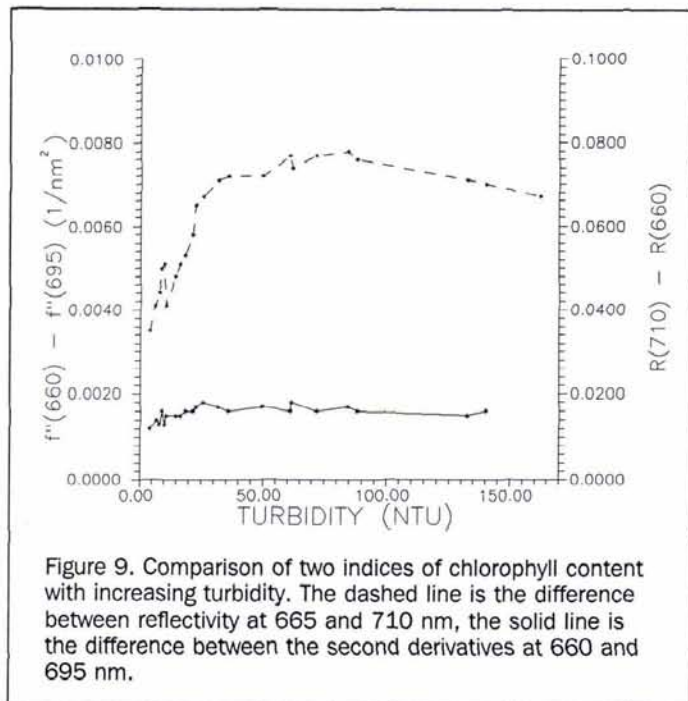


Figure 9. Comparison of two indices of chlorophyll content with increasing turbidity. The dashed line is the difference between reflectivity at 665 and 710 nm, the solid line is the difference between the second derivatives at 660 and 695 nm.

with a potentially powerful tool for determining the amount and spatial pattern of suspended materials in lakes and reservoirs. The methods outlined here furnish managers with powerful analysis techniques to fully utilize the potential of high resolution remote sensing systems for addressing these problems.

Acknowledgment

We wish to thank David W. Leavitt for deriving the seven-point numerical differentiation algorithm, and Jeffrey W. Peake, University of Nebraska at Omaha, for assistance in field data collection.

References

- Alfoldi, T., 1982. Remote sensing for water quality monitoring. *Remote Sensing for Resource Management* (C. Johannsen and J. Sanders, editors), Conservation Society of America, Ankeny, Iowa, pp. 317-328.
- American Public Health Association, 1989. *Standard Methods for the Examination of Water and Wastewater*. American Public Health Association, Washington, D.C., pp. 10-31 to 10-34.
- Curcio, J. A., and C. Petty, 1951. The near infrared absorption spectrum of liquid water. *Journal of the Optical Society of America*. 41:302-305.
- Burden, R. L., and J. D. Faires, 1989. *Numerical Analysis*, 4th ed., PWS-Kent, Boston.
- Demetriades-Shah, T. H., M. T. Steven, and J. A. Clark, 1990. High resolution derivative spectra in remote sensing. *Remote Sensing of Environment*. 33:55-64.
- DeNoyelles, F., W. D. Kettle, and D. Sinn, 1982. The response of plankton communities in experimental ponds to atrazine, the most heavily used pesticide in the United States. *Ecology*. 63:1285-1293.
- Green, G. L., and T. C. O'Hare, 1974. Derivative luminescence spectrometry. *Analytical Chemistry*. 46:2191-2196.
- Hilton, J., 1984. Airborne remote sensing for freshwater and estuarine monitoring. *Water Resources*. 18:1195-1223.
- Horn, E. M., and L. A. Morrissey, 1984. Use of Thematic Mapper for water quality assessment. *Proceedings of the Symposium on Machine Processing of Remotely Sensed Data*. West Lafayette, Indiana, pp. 244-251.
- Jensen, J., B. Kjerve, E. Ramsey, III, K. Magill, C. Medeiros, and J. Sneed, 1989. Remote sensing and numerical modeling of suspended sediment in Laguna de Terminos, Campeche, Mexico. *Remote Sensing of Environment*. 28:33-44.
- Martin, A. E., 1957. Difference and derivative spectra. *Nature*. 180:231-233.
- Quibel, G., 1991. The effect of suspended sediment on reflectance from freshwater algae. *International Journal of Remote Sensing*. 12:177-182.
- Verdin, J., 1985. Monitoring water quality conditions in a large western reservoir with Landsat imagery. *Photogrammetric Engineering & Remote Sensing*. 51:343-353.
- (Received 16 March 1992, Accepted 16 June 1992, Revised 30 July 1992)

LIST OF "LOST" CERTIFIED PHOTOGRAMMETRISTS

We no longer have valid addresses for the following Certified Photogrammetrists. If you know the whereabouts of any of the persons on this list, please contact ASPRS headquarters so we can update their records and keep them informed of all the changes in the Certification Program. Thank you.

Dewayne Blackburn
 Albert Brown
 Eugene Caudell
 Robert Denny
 Leo Ferran
 Robert Fuoco
 Franek Gajdeczka
 George Glaser
 William Grehn, Jr.
 Elwood Haynes

F.A. Hildebrand, Jr.
 James Hogan
 William Janssen
 Lawrence Johnson
 Spero Kapelas
 Francisco Milande
 Harry J. Miller
 Marinus Moojen
 Gene A. Pearl
 Sherman Rosen

Lane Schultz
 James Steckling
 Keith Syrett
 William Thomasset
 Conrad Toledo
 Robert Tracy
 Lawrence Watson
 Tad Wojenka